3-24-2012

A Learning Algorithm for Applying Cohen's Models to System Identification

Chaouki T. Abdallah

James W. Howes

Gregory L. Heileman

A Learning Algorithm for Applying Cohen's Models to System Identification*

James W. Howse Chaouki T. Abdallah Gregory L. Heileman

Department of Electrical and Computer Engineering
University of New Mexico
Albuquerque, NM 87131

Abstract

In this paper we extend the models discussed by Cohen (1992) by introducing an input term. This allows the resulting models to be utilized for system identification tasks. We prove that this model is stable in the sense that a bounded input leads to a bounded state when a minor restriction is imposed on the Lyapunov function. By employing this stability result, we are able to find a learning algorithm which guarantees convergence to a set of parameters for which the error between the model trajectories and the desired trajectories vanishes.

1 Introduction

In this paper we present a straightforward extension of the models introduced by Cohen (1992). Specifically we introduce an additional term to allow for an external input. This allows these models to be utilized for system identification tasks. By imposing a minor restriction on the Lyapunov functions constructed in Cohen (1992), we prove that this extended model is stable in the sense that a bounded input leads to a bounded state. Using this stability result and the proper model parametrization, we are able to find a learning algorithm which converges to a set of parameters which minimize the training error. Specifically the algorithm guarantees that the error between the between the model trajectories and the desired trajectories vanishes. Our learning procedure is related to one discussed in Narendra and Annaswamy (1989) for use in linear system identification. This learning procedure can also be used for associative memory applications, by setting the external inputs to zero. This allows some parameters of Cohen's memory models to be learned from examples rather than being programmed in advance.

This paper is organized as follows. In Section 2 the decomposition of dynamics into a component normal to some surface and a set of components tangent to the same surface is discussed. The learning algorithm and some theorems about its behavior are given in Section 3. In Section 4 the results of some computer simulations are presented. The proofs for all of the theorems are given in the Appendix.

2 Model Form

First some terminology will be defined. For a system of n first order ordinary differential equations, the *phase space* of the system is the n-dimensional space of all state components. A solution *trajectory* is a curve in phase space described by the differential equations for one specific starting point. At every point on a trajectory there exists a tangent vector. The space of all such tangent vectors for all possible solution trajectories constitutes the *vector field* for this system of differential equations. The operation $\|\boldsymbol{x}\|$ denotes the p-norm $(|x_1|^p + |x_2|^p + \cdots + |x_n|^p)^{\frac{1}{p}}$ of the n-dimensional vector $\boldsymbol{x}$ for some p such that $1 \leq p < \infty$, and where $|\cdot|$ is the absolute value. For the purposes of the theorems any p-norm may be

*This paper is under review for the journal *Neural Networks*.

chosen. In the simulations $p = 2$ has been chosen, so that the norm is the Euclidean distance. A *potential function* $V(\boldsymbol{x})$ is any scalar valued function of the system states $\boldsymbol{x} = [x_1, x_2, \ldots, x_n]^\dagger$ which is at least twice continuously differentiable (i.e. $V(\boldsymbol{x}) \in C^r : r \geq 2$). The operation $\boldsymbol{x}^\dagger$ denotes the transpose of the vector $\boldsymbol{x}$. If there are n components in the system state, the function $V(\boldsymbol{x})$, when plotted with respect all of the state components, defines a surface in an $(n+1)$-dimensional space, which is called the *graph* of $V(\boldsymbol{x})$.

The models considered in this paper all have the general form

$$\dot{\boldsymbol{x}} = -\boldsymbol{P}(\boldsymbol{x})\,\nabla_{\boldsymbol{x}} V(\boldsymbol{x}) + \boldsymbol{Q}(\boldsymbol{x})\,\nabla_{\boldsymbol{x}} V(\boldsymbol{x}) + \boldsymbol{h}(\boldsymbol{u}(t)), \tag{1}$$

where $\boldsymbol{P}(\boldsymbol{x})$ is a matrix function which is symmetric (i.e., $\boldsymbol{P}^\dagger = \boldsymbol{P}$) and positive definite at every point $\boldsymbol{x}$, $\boldsymbol{Q}(\boldsymbol{x})$ is a matrix function which is skew-symmetric (i.e., $\boldsymbol{Q}^\dagger = -\boldsymbol{Q}$) at every point $\boldsymbol{x}$, and where $\nabla_{\boldsymbol{x}} V(\boldsymbol{x}) = [\frac{\partial V}{\partial x_1}, \frac{\partial V}{\partial x_2}, \ldots, \frac{\partial V}{\partial x_n}]^\dagger$. The function $\boldsymbol{u}(t)$ is a time-varying input, and $\boldsymbol{h}(\cdot)$ is a possibly nonlinear transformation of the input. For this model the number and location of equilibria is determined by the function $V(\boldsymbol{x})$, while the manner in which the equilibria are approached is determined by the matrices $\boldsymbol{P}(\boldsymbol{x})$ and $\boldsymbol{Q}(\boldsymbol{x})$. When $\boldsymbol{h}(\boldsymbol{u}(t)) = \boldsymbol{0}$, the critical points of $V(\boldsymbol{x})$ are the only equilibria of this system. If the graph of the potential function $V(\boldsymbol{x})$ is ① bounded below (i.e., $V(\boldsymbol{x}) > \mathcal{M}\ \forall\ \boldsymbol{x} \in \mathbb{R}^n$, where $\mathcal{M}$ is a constant), ② radially unbounded (i.e., $\lim_{\|\boldsymbol{x}\| \to \infty} V(\boldsymbol{x}) \to \infty$) , and ③ has only a finite number of isolated critical points (i.e., in some neighborhood of every point where $\nabla_{\boldsymbol{x}} V(\boldsymbol{x}) = \boldsymbol{0}$ there are no other points where the gradient vanishes), then for $\boldsymbol{h}(\boldsymbol{u}(t)) = \boldsymbol{0}$ the system in Equation (1) satisfies the conditions of Theorem 10 in Cohen (1992). Therefore the system will converge to one of the critical points of $V(\boldsymbol{x})$ for all initial conditions. The systems in Equation (1) are a non-autonomous special case of the gradient-like systems presented in Franks (1982). This means that they are not able to represent arbitrary dynamics. Note that if the second term on the right hand side of Equation (1) is replaced by the term $\sum_{i=2}^{n} \boldsymbol{Q}_i(\boldsymbol{x})\,\nabla_{\boldsymbol{x}} H_i(\boldsymbol{x})$, where $H_i(\boldsymbol{x})$ are in general different potential functions, then the resulting system *can* describe arbitrary dynamics. Specifically, Mendes and Duarte (1981) show that any vector field $\boldsymbol{f}$ on a manifold $\mathcal{M}$ can be *locally* decomposed into the sum of one gradient system and $(n-1)$ Hamiltonian systems, where n is the local dimension of the manifold.

3 The Learning Rule

In this section we introduce a learning rule for the systems in Equation (1). If it is assumed that the locations of the equilibria are known, then a potential function which has these critical points can be constructed using either of the two methods discussed in Cohen (1992). The problem of system identification is thereby reduced to the problem of parameterizing the matrices $\boldsymbol{P}(\boldsymbol{x})$ and $\boldsymbol{Q}(\boldsymbol{x})$ and finding the parameter values which cause this model to best emulate the actual system. If the elements $\boldsymbol{P}(\boldsymbol{x})$ and $\boldsymbol{Q}(\boldsymbol{x})$ are correctly chosen, then a learning rule can be designed which makes the model dynamics converge to that of the actual system.

Specifically, choose each element of these matrices to have the form

$$P_{rs} = \sum_{i=1}^{n} \sum_{j=0}^{l-1} \xi_{rsij}\, \vartheta_j(x_i) \qquad \text{and} \qquad Q_{rs} = \sum_{i=1}^{n} \sum_{j=0}^{l-1} \lambda_{rsij}\, \varrho_j(x_i), \tag{2}$$

where $\{\vartheta_0(x_i), \vartheta_1(x_i), \ldots, \vartheta_{l-1}(x_i)\}$ and $\{\varrho_0(x_i), \varrho_1(x_i), \ldots, \varrho_{l-1}(x_i)\}$ are a set of l orthogonal polynomials which depend on the state x_i. There is a set of such polynomials for every state x_i, $i = 1, 2, \ldots, n$. The constants ξ_{rsij} and λ_{rsij} determine the contribution of the jth polynomial which depends on the ith state to the value of P_{rs} and Q_{rs} respectively. In this case the dynamics in Equation (1) become

$$\dot{\boldsymbol{x}} = \sum_{i=1}^{n} \sum_{j=0}^{l-1} \left\{ \boldsymbol{\Xi}_{ij} \left[\vartheta_j(x_i)\, \nabla_{\boldsymbol{x}} V(\boldsymbol{x}) \right] + \boldsymbol{\Lambda}_{ij} \left[\varrho_j(x_i)\, \nabla_{\boldsymbol{x}} V(\boldsymbol{x}) \right] \right\} + \boldsymbol{\Upsilon}\, \boldsymbol{g}(\boldsymbol{u}(t)) = \boldsymbol{f}(\boldsymbol{x}, \boldsymbol{\xi}, \boldsymbol{\lambda}, \boldsymbol{\upsilon}, t) \tag{3}$$

where $\boldsymbol{\Xi}_{ij}$ and $\boldsymbol{\Lambda}_{ij}$ are the $(n \times n)$ matrices of all values ξ_{rsij} and λ_{rsij} respectively, which have the same value of i and j. This system has m inputs, which may explicitly depend on time, that are represented by

the $\mathfrak{m}$-element vector function $\boldsymbol{u}(t)$. The $\mathfrak{m}$-element vector function $\boldsymbol{g}(\cdot)$ is a smooth, possibly nonlinear, transformation of the input function. The matrix $\boldsymbol{\Upsilon}$ is an $(\mathfrak{n} \times \mathfrak{m})$ parameter matrix which determines how much of input $s \in \{1, \ldots, \mathfrak{m}\}$ effects state $r \in \{1, \ldots, \mathfrak{n}\}$. So the dynamics depend on the system states $\boldsymbol{x}$ and all of the parameters $\boldsymbol{\xi} = [\xi_{rsij}]^\dagger : r, s, i = 1, \ldots, \mathfrak{n},\ j = 0, \ldots, \mathfrak{l}-1$, $\boldsymbol{\lambda} = [\lambda_{rsij}]^\dagger : r, s, i = 1, \ldots, \mathfrak{n},\ j = 0, \ldots, \mathfrak{l}-1$ and $\boldsymbol{\upsilon} = [\upsilon_{rs}]^\dagger : r = 1, \ldots, \mathfrak{n},\ s = 1, \ldots, \mathfrak{m}$.

The dynamics given by Equation (3) are a model of the actual system dynamics. Using this model and samples of the actual system states, an estimator for the states of the actual system can be designed. The dynamics of this state estimator are

$$\dot{\hat{\boldsymbol{x}}} = \boldsymbol{\mathcal{R}}_s \, (\hat{\boldsymbol{x}} - \boldsymbol{x}) + \boldsymbol{f}(\boldsymbol{x}, \boldsymbol{\xi}, \boldsymbol{\lambda}, \boldsymbol{\upsilon}, t) \tag{4}$$

where $\boldsymbol{x}$ is a sample of the actual system states. The term $\boldsymbol{\mathcal{R}}_s$ is a matrix of real constants whose eigenvalues must all be negative. This means that $\hat{\boldsymbol{x}}$ is an estimate of the actual system states which depends on the form of the model $\boldsymbol{f}(\boldsymbol{x}, \boldsymbol{\xi}, \boldsymbol{\lambda}, \boldsymbol{\upsilon}, t)$. The goal is to find a set of parameters $\boldsymbol{\xi}$, $\boldsymbol{\lambda}$ and $\boldsymbol{\upsilon}$ which cause the error $(\hat{\boldsymbol{x}} - \boldsymbol{x})$ to vanish. The dynamics of a parameter estimator which accomplishes this are

$$\begin{aligned}
\dot{\boldsymbol{\Xi}}_{ij} &= -\boldsymbol{\mathcal{R}}_p \, (\hat{\boldsymbol{x}} - \boldsymbol{x}) \left[\vartheta_j(x_i) \, \nabla_{\boldsymbol{x}} V(\boldsymbol{x})\right]^\dagger \ \ \forall \ \ i = 1, \ldots, \mathfrak{n},\ \ j = 0, \ldots, \mathfrak{l}-1 \\
\dot{\boldsymbol{\Lambda}}_{ij} &= -\boldsymbol{\mathcal{R}}_p \, (\hat{\boldsymbol{x}} - \boldsymbol{x}) \left[\varrho_j(x_i) \, \nabla_{\boldsymbol{x}} V(\boldsymbol{x})\right]^\dagger \ \ \forall \ \ i = 1, \ldots, \mathfrak{n},\ \ j = 0, \ldots, \mathfrak{l}-1 \\
\dot{\boldsymbol{\Upsilon}} &= -\boldsymbol{\mathcal{R}}_p \, (\hat{\boldsymbol{x}} - \boldsymbol{x}) \left[\boldsymbol{g}(\boldsymbol{u}(t))\right]^\dagger,
\end{aligned} \tag{5}$$

where $\boldsymbol{\mathcal{R}}_p$ is a matrix of real constants which is symmetric and positive definite. Note that the term $(\hat{\boldsymbol{x}} - \boldsymbol{x}) \, [\vartheta_j(x_i) \, \nabla_{\boldsymbol{x}} V(\boldsymbol{x})]^\dagger$ is the outer product of $\mathfrak{n}$-dimensional vectors, hence the result is an $(\mathfrak{n} \times \mathfrak{n})$ matrix. Likewise the terms $(\hat{\boldsymbol{x}} - \boldsymbol{x}) \, [\varrho_j(x_i) \, \nabla_{\boldsymbol{x}} V(\boldsymbol{x})]^\dagger$ and $(\hat{\boldsymbol{x}} - \boldsymbol{x}) \, [\boldsymbol{g}(\boldsymbol{u}(t))]^\dagger$ are also outer products. The following theorem shows that the system of differential equations defined by Equations (3), (4) and (5) converge to a set of parameters such that the error $(\hat{\boldsymbol{x}} - \boldsymbol{x})$ between the estimated and target trajectories vanishes.

Theorem 3.1. *Given the model system*

$$\dot{\boldsymbol{x}} = \sum_{i=1}^{\mathfrak{k}} \boldsymbol{A}_i \, \boldsymbol{f}_i(\boldsymbol{x}) + \boldsymbol{B} \, \boldsymbol{g}\big(\boldsymbol{u}(t)\big) \tag{6}$$

where $\boldsymbol{A}_i \in \mathbb{R}^{\mathfrak{n} \times \mathfrak{n}}$ and $\boldsymbol{B} \in \mathbb{R}^{\mathfrak{n} \times \mathfrak{m}}$ are unknown matrices, and $\boldsymbol{f}_i : \mathbb{R}^{\mathfrak{n}} \to \mathbb{R}^{\mathfrak{n}}$, $\boldsymbol{f}_i \in C^1$ and $\boldsymbol{g} : \mathbb{R}^{\mathfrak{m}} \to \mathbb{R}^{\mathfrak{m}}$, $\boldsymbol{g} \in C^1$ are known functions such that $\|\boldsymbol{u}(t)\| \leq \mathcal{U}$ for some $\mathcal{U} > 0$ implies $\|\boldsymbol{x}(t)\| \leq \mathcal{S}_u$ for some $\mathcal{S}_u > 0$ (i.e., bounded inputs imply bounded solutions). Choose a state estimator of the form

$$\dot{\hat{\boldsymbol{x}}} = \boldsymbol{\mathcal{R}}_s \, (\hat{\boldsymbol{x}} - \boldsymbol{x}) + \sum_{i=1}^{\mathfrak{k}} \hat{\boldsymbol{A}}_i \, \boldsymbol{f}_i(\boldsymbol{x}) + \hat{\boldsymbol{B}} \, \boldsymbol{g}\big(\boldsymbol{u}(t)\big) \tag{7}$$

where $\boldsymbol{\mathcal{R}}_s \in \mathbb{R}^{\mathfrak{n} \times \mathfrak{n}}$ is a matrix whose eigenvalues must all be in the left half plane, and $\hat{\boldsymbol{A}}_i$ and $\hat{\boldsymbol{B}}$ are the estimates of the actual parameters. Choose parameter estimators of the form

$$\begin{aligned}
\dot{\hat{\boldsymbol{A}}}_i &= -\boldsymbol{\mathcal{R}}_p \, (\hat{\boldsymbol{x}} - \boldsymbol{x}) \left(\boldsymbol{f}_i(\boldsymbol{x})\right)^\dagger \ \ \forall \ \ i = 1, \ldots, \mathfrak{k} \\
\dot{\hat{\boldsymbol{B}}} &= -\boldsymbol{\mathcal{R}}_p \, (\hat{\boldsymbol{x}} - \boldsymbol{x}) \left(\boldsymbol{g}(\boldsymbol{u}(t))\right)^\dagger
\end{aligned} \tag{8}$$

where $\boldsymbol{\mathcal{R}}_p \in \mathbb{R}^{\mathfrak{n} \times \mathfrak{n}}$ is the matrix which is a solution of the equation $\boldsymbol{\mathcal{R}}_p \, \boldsymbol{\mathcal{R}}_s + \boldsymbol{\mathcal{R}}_s^\dagger \, \boldsymbol{\mathcal{R}}_p = -\boldsymbol{Q}_0$. The matrix $\boldsymbol{Q}_0 \in \mathbb{R}^{\mathfrak{n} \times \mathfrak{n}}$ must be symmetric and positive definite. For these choices of state and parameter estimators $\lim_{t \to \infty} (\hat{\boldsymbol{x}} - \boldsymbol{x}) = \boldsymbol{0}$ for all initial conditions. Furthermore, this remains true if any *of the elements of $\hat{\boldsymbol{A}}_i$ or $\hat{\boldsymbol{B}}$ are set to 0, or if any of these matrices are restricted to being symmetric or skew-symmetric.*

The proof of this theorem is quite standard and appears in Howse (1995). Notice that $(\hat{\boldsymbol{x}} - \boldsymbol{x}) \, (\cdot)^\dagger$ denotes an outer product. Note that convergence of the parameter estimates to the actual parameter values is not guaranteed by this theorem. Since Equations (3), (4), and (5) are in the form of Equations (6), (7), and

(8) respectively, Theorem 3.1 implies that the parameter estimates produced by Equation (5) cause the state estimates in Equation (4) to converge to the actual state values.

Theorem 3.1 is based on the assumption that the state vector in Equation (6) is bounded if the input $\boldsymbol{u}(t)$ is bounded (i.e., BIBS stability). If $\boldsymbol{f}_i(\cdot)$ and $\boldsymbol{g}(\cdot)$ are linear functions, the resulting linear system is BIBS stable if it is asymptotically stable when $\boldsymbol{u}(t) = \boldsymbol{0}$, as shown by Willems (1970). However, it was shown by Varaiya and Liu (1966) that asymptotic stability of the zero input case alone does not guarantee BIBS stability for nonlinear systems. This means that in order to determine the boundedness of the solutions $\boldsymbol{x}(t)$ of Equation (3), a non-autonomous nonlinear system must be considered. In general this can be quite difficult, but for systems of this form, results in LaSalle and Lefschetz (1961) can be used to prove the following theorem.

Theorem 3.2. *Given the dynamical system*

$$\dot{\boldsymbol{x}} = -\boldsymbol{P}(\boldsymbol{x})\,\nabla_{\boldsymbol{x}} V(\boldsymbol{x}) + \boldsymbol{Q}(\boldsymbol{x})\,\nabla_{\boldsymbol{x}} V(\boldsymbol{x}) + \boldsymbol{h}(\boldsymbol{u}(t)), \tag{9}$$

where $V : \mathbb{R}^{\mathfrak{n}} \to \mathbb{R}$, $V \in C^2$ is the potential function, $\boldsymbol{h} : \mathbb{R}^{\mathfrak{m}} \to \mathbb{R}^{\mathfrak{n}}$, $\boldsymbol{h} \in C^1$, and $\boldsymbol{u} : \mathbb{R} \to \mathbb{R}^{\mathfrak{m}}$, $\boldsymbol{u} \in C^1$ is a time varying input function. The matrix function $\boldsymbol{P} : \mathbb{R}^{\mathfrak{n}} \to \mathbb{R}^{\mathfrak{n}\times\mathfrak{n}}$, $\boldsymbol{P} \in C^1$ is symmetric positive definite, and $\boldsymbol{Q} : \mathbb{R}^{\mathfrak{n}} \to \mathbb{R}^{\mathfrak{n}\times\mathfrak{n}}$, $\boldsymbol{Q} \in C^1$ is skew-symmetric. Furthermore, $V(\boldsymbol{x}) \geq 0$ for all $\boldsymbol{x}$, and there exists an $\mathcal{F}_u > 0$, such that for $\|\boldsymbol{x}\| > \mathcal{F}_u$, $\|\nabla_{\boldsymbol{x}} V(\boldsymbol{x})\| \geq \mathcal{K}_u$ for some $\mathcal{K}_u > 0$ (i.e., the length of $\nabla_{\boldsymbol{x}} V(\boldsymbol{x})$ has a non-zero lower bound). Also there exists a $\mathcal{U} > 0$ such that $\|\boldsymbol{u}(t)\| \leq \mathcal{U}$. If all of the above conditions are satisfied, then there exists $\mathcal{S}_u > 0$ such that corresponding to each solution $\boldsymbol{x}(t)$ of Equation (9) there is a $\mathcal{T} > 0$ with the property that $\|\boldsymbol{x}(t)\| \leq \mathcal{S}_u$ for all $t > \mathcal{T}$ (i.e., the solutions $\boldsymbol{x}(t)$ of Equation (9) are ultimately bounded).

The proof of this theorem appears in the Appendix. Note that the system has $\mathfrak{n}$ states and $\mathfrak{m}$ inputs, where $\mathfrak{m}$ and $\mathfrak{n}$ may differ. This theorem states that if there is a region outside which the length of $\nabla_{\boldsymbol{x}} V(\boldsymbol{x})$ has a non-zero lower bound, then all solutions to Equation (9) are ultimately bounded provided that the norm of the input signal $\|\boldsymbol{u}(t)\|$ is bounded. It turns out that $\mathcal{K}_u$ depends on $\mathcal{U}$, the upper bound on $\|\boldsymbol{u}(t)\|$ (see the proof). So if the system is to accommodate arbitrarily large inputs, there must be a region $\|\boldsymbol{x}\| > \mathcal{F}_m$ in which $\|\nabla_{\boldsymbol{x}} V(\boldsymbol{x})\|$ is strictly increasing (i.e., $\|\boldsymbol{x}_1\| > \|\boldsymbol{x}_2\| \Rightarrow \|\nabla_{\boldsymbol{x}} V(\boldsymbol{x}_1)\| > \|\nabla_{\boldsymbol{x}} V(\boldsymbol{x}_2)\|$). If this is the case, then for any $\mathcal{K}_u$, and hence any $\mathcal{U}$, there exists a region $\|\boldsymbol{x}\| > \mathcal{F}_u \geq \mathcal{F}_m$ in which $\|\nabla_{\boldsymbol{x}} V(\boldsymbol{x})\| \geq \mathcal{K}_u$. The condition $\|\nabla_{\boldsymbol{x}} V(\boldsymbol{x})\| \geq \mathcal{K}_u$ implies that $V(\boldsymbol{x}) \geq \mathcal{K}_u \|\boldsymbol{x}\|$ which means that $V(\boldsymbol{x})$ is radially unbounded, but not necessarily convex or even increasing. It is not obvious what condition on $V(\boldsymbol{x})$ implies $\|\nabla_{\boldsymbol{x}} V(\boldsymbol{x})\| \geq \mathcal{K}_u$, for instance $V(\boldsymbol{x}) \geq \mathcal{K}_u \|\boldsymbol{x}\| \not\Rightarrow \|\nabla_{\boldsymbol{x}} V(\boldsymbol{x})\| \geq \mathcal{K}_u$. An interesting converse to this theorem can also be proven. If $V(\boldsymbol{x})$ is continuous, lower bounded, and has some region $\|\boldsymbol{x}\| > \mathcal{F}_u$ where $\|\nabla_{\boldsymbol{x}} V(\boldsymbol{x})\| \geq \mathcal{K}_u$, then there exists some region (or possibly regions) $\|\boldsymbol{x} - \boldsymbol{C}\| < \mathcal{F}_l$ wherein $\|\nabla_{\boldsymbol{x}} V(\boldsymbol{x})\| \leq \mathcal{K}_l$ for some $\mathcal{F}_l, \mathcal{K}_l > 0$. In this region it can be shown that $\dot{V}(\boldsymbol{x})$ is always positive, hence this region is unstable and the system will eventually leave it. Therefore the solutions of Equation (9) have both an ultimate upper bound and an ultimate lower bound, so for $t > \mathcal{T}$, $\mathcal{S}_l \leq \|\boldsymbol{x}(t)\| \leq \mathcal{S}_u$ for some $\mathcal{S}_u \geq \mathcal{S}_l > 0$.

As previously stated, Theorem 3.1 does not guarantee the convergence of the parameter estimates to the actual parameter values. This issue has been widely addressed in the adaptive identification and control literature, as discussed in Narendra and Annaswamy (1987). It was determined that if the signals within the adaptive system possessed certain properties, then the origin of the system was globally uniformly asymptotically stable. This guarantees the convergence of the parameter estimates. Signals with these properties are said to be *persistently exciting* by Narendra and Annaswamy (1987). Intuitively, persistent excitation means that the input is rich enough to excite all the modes of the system being considered. For linear systems persistent excitation becomes a condition on the input signal alone, since a linear system can not generate frequency modes. For a nonlinear system the condition must be on both the input signal and the internal signals of the system, since nonlinear systems can generate new frequency modes. Using results from Morgan and Narendra (1977) the following theorem can be proven for the identification system defined by Equations (6), (7) and (8).

Theorem 3.3. *Given the model system*

$$\dot{\boldsymbol{x}} = \sum_{i=1}^{\mathfrak{k}} \boldsymbol{A}_i\, \mathcal{F}_i(\boldsymbol{x})\, \nabla_{\boldsymbol{x}} V(\boldsymbol{x}) + \boldsymbol{B}\, \boldsymbol{g}(\boldsymbol{u}(t)), \tag{10}$$

where $\mathcal{F}_i : \mathbb{R}^{\mathrm{d}} \to \mathbb{R}$, $\mathrm{d} \leq \mathrm{n}$ *(i.e.,* $\mathcal{F}_i(\cdot)$ *may be a function of some subset of the elements in the state vector* $\boldsymbol{x}$*),* $\mathcal{F}_i \in C^1$*. Let all* $\boldsymbol{A}_i \in \mathbb{R}^{\mathrm{n}\times\mathrm{n}}$ *be either symmetric positive definite or skew-symmetric and let Equation* (10) *satisfy all of the conditions in Theorems* 3.1 *and* 3.2*. Define the error functions* $\boldsymbol{e} = \hat{\boldsymbol{x}} - \boldsymbol{x}$*,* $\boldsymbol{\Phi}_i = \hat{\boldsymbol{A}}_i - \boldsymbol{A}_i$*, and* $\boldsymbol{\Psi} = \hat{\boldsymbol{B}} - \boldsymbol{B}$*. From Equations* (7) *and* (8) *the state and parameter error dynamics are*

$$\begin{aligned}
\dot{\boldsymbol{e}} &= \dot{\hat{\boldsymbol{x}}} - \dot{\boldsymbol{x}} = \boldsymbol{\mathcal{R}}_s\, \boldsymbol{e} + \sum_{i=1}^{\mathrm{k}} \boldsymbol{\Phi}_i\, \mathcal{F}_i(\boldsymbol{x})\, \nabla_{\boldsymbol{x}} V(\boldsymbol{x}) + \boldsymbol{\Psi}\, \boldsymbol{g}(\boldsymbol{u}(t)), \\
\dot{\boldsymbol{\Phi}}_i &= \dot{\hat{\boldsymbol{A}}}_i - \dot{\boldsymbol{A}}_i = -\boldsymbol{\mathcal{R}}_p\, \boldsymbol{e}\, [\mathcal{F}_i(\boldsymbol{x})\, \nabla_{\boldsymbol{x}} V(\boldsymbol{x})]^{\dagger}\,, \\
\dot{\boldsymbol{\Psi}} &= \dot{\hat{\boldsymbol{B}}} - \dot{\boldsymbol{B}} = -\boldsymbol{\mathcal{R}}_p\, \boldsymbol{e}\, \boldsymbol{g}(\boldsymbol{u}(t))^{\dagger},
\end{aligned} \tag{11}$$

Let $\|\dot{\boldsymbol{u}}(t)\| \leq \mathcal{D}$ *for some* $\mathcal{D} > 0$*, and let there exist positive constants* t_0*,* $\mathcal{T}$*, and* ϵ *such that for every unit vector* $\boldsymbol{w} \in \mathbb{R}^{\mathrm{n}+\mathrm{m}}$

$$\frac{1}{\mathcal{T}} \int_t^{t+\mathcal{T}} \left\| \left\{ [\mathcal{F}_1(\boldsymbol{x}(\tau)) + \mathcal{F}_2(\boldsymbol{x}(\tau)) + \cdots + \mathcal{F}_{\mathrm{k}}(\boldsymbol{x}(\tau))]\ \nabla_{\boldsymbol{x}} V(\boldsymbol{x}(\tau))^{\dagger}\ \boldsymbol{g}(\boldsymbol{u}(\tau))^{\dagger} \right\} \boldsymbol{w} \right\|\, d\tau \geq \epsilon \quad \forall \quad t \geq t_0. \tag{12}$$

Then the equilibrium point $\boldsymbol{e} = \boldsymbol{0}$*,* $\boldsymbol{\Phi}_i = \mathbf{O}$*,* $\boldsymbol{\Psi} = \mathbf{O}$ *is globally uniformly asymptotically stable.*

The proof of this theorem follows almost immediately from Theorem 4 in Morgan and Narendra (1977). Note that Equation (11) is non-autonomous due to the input term. Also, the choice of parameter error dynamics is dictated by the fact that the actual parameters $\boldsymbol{A}_i$ and $\boldsymbol{B}$ are assumed to be unknown constants. This theorem gives a condition on the internal signals and inputs of the system in Equation (11) which guarantee convergence of the parameter estimates to their actual values. The intuitive meaning of this condition is far from obvious. In part it means that there is a time interval $\mathcal{T}$ over which the vector $\left\{ \left[\sum_{i=1}^{\mathrm{k}} \mathcal{F}_i(\boldsymbol{x})\right]\ \nabla_{\boldsymbol{x}} V(\boldsymbol{x})\ \boldsymbol{g}(\boldsymbol{u}(t)) \right\}$ points in all directions with sufficient length as t takes on values in the interval. Notice that in Equation (3) the form of $\mathcal{F}_i(\boldsymbol{x})$ is $\omega_j(x_i)$, $j = 0, 1, \ldots, \mathrm{l}-1$, $i = 1, 2, \ldots, \mathrm{n}$ where $\omega_j(\cdot)$ is the jth member of a set of l orthogonal polynomials, and $x_i \in \{x_1, x_2, \ldots, x_{\mathrm{n}}\}$.

4 Simulation Results

Now an example is presented in which the parameters of the model in Equation (3) are learned, using the training rule in Equations (4) and (5), on one input signal and then are tested on a different input signal. The actual system has three equilibrium points, two stable points located at $(1, 3)$ and $(3, 5)$, and a saddle point located at $(2 - \frac{\sqrt{3}}{3}, 4 + \frac{\sqrt{3}}{3})$. In this example the dynamics of both the actual system and the model are given by

$$\begin{pmatrix} \dot{x}_1 \\ \dot{x}_2 \end{pmatrix} = -\begin{pmatrix} \mathcal{A}_1 + \mathcal{A}_2\, x_1^2 + \mathcal{A}_3\, x_2^2 & 0 \\ 0 & \mathcal{A}_4 + \mathcal{A}_5\, x_1^2 + \mathcal{A}_6\, x_2^2 \end{pmatrix} \begin{pmatrix} \dfrac{\partial V}{\partial x_1} \\ \dfrac{\partial V}{\partial x_2} \end{pmatrix} + \begin{pmatrix} 0 & -\{\mathcal{A}_7 + \mathcal{A}_8\, x_1 + \mathcal{A}_9\, x_2\} \\ \mathcal{A}_7 + \mathcal{A}_8\, x_1 + \mathcal{A}_9\, x_2 & 0 \end{pmatrix} \begin{pmatrix} \dfrac{\partial V}{\partial x_1} \\ \dfrac{\partial V}{\partial x_2} \end{pmatrix} + \begin{pmatrix} \mathcal{A}_{10} \\ 0 \end{pmatrix} u, \tag{13}$$

where u is a time varying input. For the actual system the parameter values were $\mathcal{A}_1 = \mathcal{A}_4 = -4$, $\mathcal{A}_2 = \mathcal{A}_5 = -2$, $\mathcal{A}_3 = \mathcal{A}_6 = -1$, $\mathcal{A}_7 = 1$, $\mathcal{A}_8 = 3$, $\mathcal{A}_9 = 5$, and $\mathcal{A}_{10} = 1$. In the model the 10 elements $\mathcal{A}_i$ are treated as the unknown parameters which must be learned. Note that the first matrix function is positive definite if the parameters $\mathcal{A}_1$–$\mathcal{A}_6$ are all positive valued. The second matrix function is skew-symmetric for all values of $\mathcal{A}_7$–$\mathcal{A}_9$. For this particular system $\nabla_{\boldsymbol{x}} V(\boldsymbol{x})$ is

$$\begin{pmatrix} \dfrac{\partial V}{\partial x_1} \\ \dfrac{\partial V}{\partial x_2} \end{pmatrix} = \begin{pmatrix} 576\, x_1^5 - 5379.45\, x_1^4 + 19742.3\, x_1^3 - 35767.5\, x_1^2 + 31999.2\, x_1 - 24\, x_1\, x_2 + 47\, x_2 - 11239.5 \\ -12\, x_1^2 + 47\, x_1 + x_2 - 38 \end{pmatrix}. \tag{14}$$

It is relatively easy to show that for this example, $\|\nabla_{\boldsymbol{x}} V(\boldsymbol{x})\|$ is eventually strictly increasing as illustrated in Figure 1. The function is actually increasing in the X-shaped trough seen in the figure, but at a much

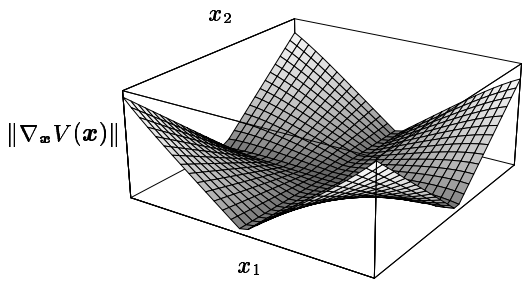

Figure 1: The graph of the norm of the gradient $\|\nabla_{\boldsymbol{x}} V(\boldsymbol{x})\|$ for the system defined in Equation (14).

slower rate than in the surrounding areas. This means that for *any* bounded input, the system defined by Equations (13) and (14) satisfies the conditions in Theorem 3.2 and therefore has ultimately bounded solutions. The two input signals used for training and testing were $u_1(t) = 10000\left(\sin\frac{1}{3}1000\,t + \sin\frac{2}{3}1000\,t\right)$ and $u_2(t) = 5000\sin 1000\,t$. The phase space responses of the actual system to the inputs u_1 and u_2 are shown by the solid curves in Figures 4(b) and 4(a) respectively. Note that both of these inputs produce a periodic attractor in the phase space of Equation (13).

In order to evaluate the effectiveness of the learning algorithm the Euclidean distance between the actual and learned state and parameter values was computed and plotted versus time. The results are shown in Figure 2. Figure 2(a) shows these statistics when training with input u_1, while Figure 2(b) shows the same

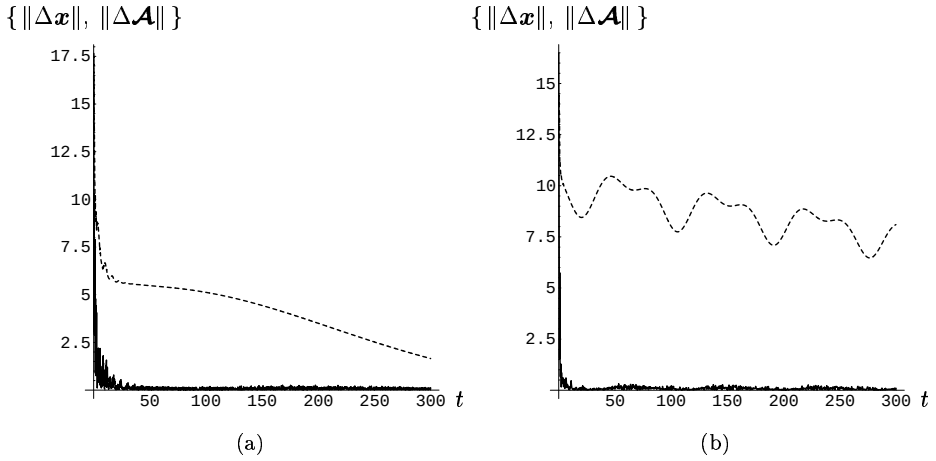

Figure 2: (a) The state and parameter errors for training using input signal u_1. The solid curve is the Euclidean distance (i.e., $\sqrt{\sum_{i=1}^{2}\hat{x}_i - x_i}$) between the state estimates and the actual states as a function of time. The dashed curve shows the distance (i.e., $\sqrt{\sum_{i=1}^{10}\hat{\mathcal{A}}_i - \mathcal{A}_i}$) between the estimated and actual parameter values versus time.
(b) The state and parameter errors for training using input signal u_2.

statistics for input u_2. The solid curves are the Euclidean distance between the learned and actual system states, and the dashed curves are the distance between the learned and actual parameter values. These statistics have two noteworthy features. First, the error between the learned and desired states quickly converges to very small values, regardless of how well the actual parameters are learned. This result was guaranteed by Theorem 3.1. Second, the minimum error between the learned and desired parameters is much lower when the system is trained with input u_1. Specifically the minimum parameter error for input u_1 is 1.65, while for input u_2 it is 6.47. Intuitively this is because input u_1 excites more frequency modes of the system than input u_2. Notice that the parameter error curve in Figure 2(a) appears to be eventually monotonically decreasing. So it seems reasonable to conclude that for input u_1 the parameter estimates eventually converge to the actual parameter values. The same conclusion also seems to justified for input u_2 since the envelope of the parameter error curve in Figure 2(b) decreases with time. These observations illustrate the relationship between parameter convergence and persistent excitation that was addressed in Theorem 3.3. Recall that in a nonlinear system the frequency modes excited by a given input do not

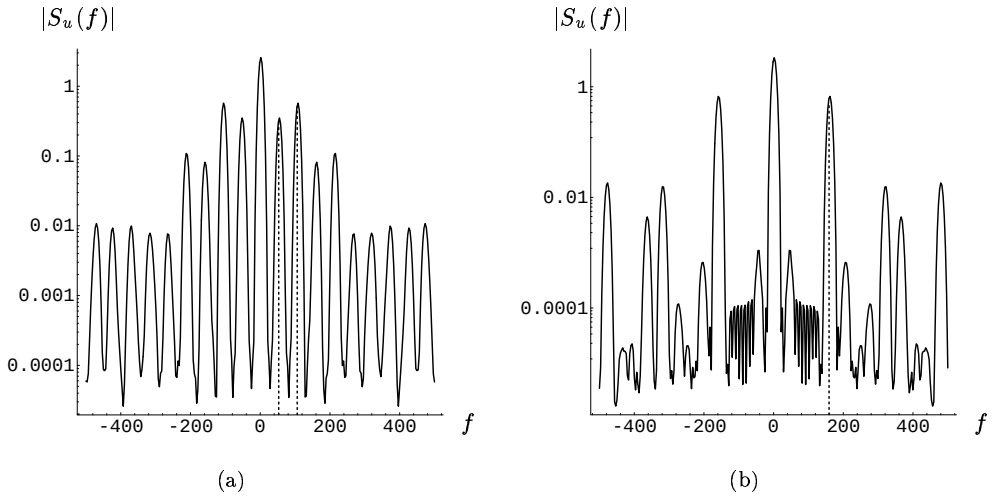

Figure 3: (a) The power spectral density versus frequency of the state $x_1(t)$ when Equation (13) is driven by input $u_1(t)$. The dashed lines represent the two frequencies present in the input.
(b) The power spectral density of $x_1(t)$ for input $u_2(t)$. The dashed line represents the one frequency present in the input.

depend solely on the input because the system can generate frequencies not present in the input. These conclusions are further supported by the plots of the power spectrum of state $x_1(t)$ for each input, shown in Figure 3. Figure 3(a) shows the power spectrum for input $u_1(t)$, while Figure 3(b) shows it for input $u_2(t)$. The dashed lines show the frequencies present in the input signal. Note that the DC peak in both power spectra is due to the fact that neither of the periodic structures generated by these inputs is centered at the origin. These plots have two features of note. First, input u_1 clearly excites more system modes than input u_2. This partially explains why the parameter convergence for u_1 is better than for u_2, as shown in Figure 2. Second, both inputs excite modes in the system which are at frequencies *not* present in the input. This is a result of the nonlinearities in Equation (13). The large number of spectral components supports the conclusion that for this particular system both u_1 and u_2 are persistently exciting.

The quality of the learned parameters can be qualitatively judged by comparing the phase plots using the learned and actual parameters for each input, as shown in Figure 4. In Figure 4(a) the system was trained

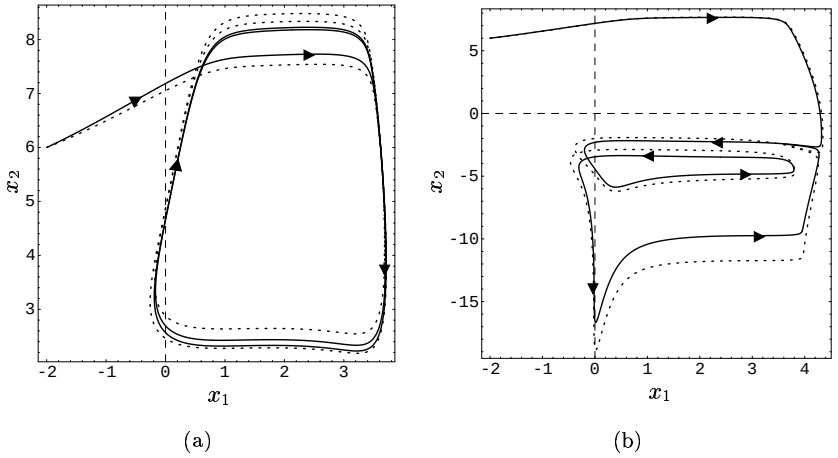

Figure 4: (a) A phase plot of the system response when trained with input u_1 and tested with input u_2. The solid line is the response to the test input using the actual parameters. The dotted line is the system response using the learned parameters.
(b) A phase plot of the system response when trained with input u_2 and tested with input u_1.

using input u_1 and tested with input u_2, while in Figure 4(b) the situation was reversed. The solid curves are the system response using the actual parameter values, and the dashed curves are the response using

the final values of the learned parameters. The Euclidean distance between the target and test trajectories in Figure 4(a) is in the range $(0, 0.64)$ with a mean distance of 0.21 and a standard deviation of 0.14. The distance between the the target and test trajectories in Figure 4(b) is in the range $(0, 4.53)$ with a mean distance of 0.98 and a standard deviation of 1.35. Qualitatively, both sets of learned parameters give an accurate response for non-training inputs. Note that even when the error between the learned and actual parameters is large, the periodic attractor resulting from the learned parameters appears to have the same "shape" as that for the actual parameters.

5 Conclusion

In this paper we present an extension to the models of Cohen (1992) which allows them to be used for system identification. By imposing a minor restriction on the potential function in Equation (1) we are able to prove that these systems are bounded-input bounded-state stable. We then use this stability result to develop a convergent learning algorithm for the model parameters. This algorithm is guaranteed to converge to a set of parameter values for which the error between the learned and desired trajectories vanishes. We also present a condition for the persistent excitation of the inputs and the system states.

The first two terms on the right hand side of Equation (1) can be combined by letting $\boldsymbol{M}(\boldsymbol{x}) = -\boldsymbol{P}(\boldsymbol{x}) + \boldsymbol{Q}(\boldsymbol{x})$. An alternate way to construct systems which satisfy Theorem 10 in Cohen (1992) is to construct the matrix $\boldsymbol{M}(\boldsymbol{x})$ such that the first row is always along $-\nabla_{\boldsymbol{x}} V(\boldsymbol{x})$ and all rows are mutually orthogonal. One way to construct this matrix is to find $-\nabla_{\boldsymbol{x}} V(\boldsymbol{x})$ at each point $\boldsymbol{x}$, and then use Gram-Schmidt orthogonalization to find the remaining rows. However, it would be far more elegant to find a global construction that could be performed *a priori*. A significant unanswered question about the models in Equation (1) is how large a subset of dynamical systems they can approximate. If $V(\boldsymbol{x})$ is constructed using either of the two techniques presented in Cohen (1992), then it is shown in that paper that the resulting systems can not even describe all gradient systems. Even if $V(\boldsymbol{x})$ is arbitrary, the results in our paper do not allow all gradient systems to be learned because only the transient behavior represented by the matrix functions $\boldsymbol{P}(\boldsymbol{x})$ and $\boldsymbol{Q}(\boldsymbol{x})$ is being modeled. Clearly, in order to model the behavior of a general system, the long term behavior represented by the potential function $V(\boldsymbol{x})$ must also be learned from data. Since finding asymptotically stable structures in data is usually straightforward, learning $V(\boldsymbol{x})$ from data may appear fairly trivial at first glance. However, unstable structures can have a significant impact on the system dynamics, and these are in general very difficult to locate. We are currently investigating constructive algorithms to synthesize the potential function $V(\boldsymbol{x})$. This would lead to a two-stage learning procedure in which the algorithm presented here is used to learn the transient behavior (i.e., $\boldsymbol{P}(\boldsymbol{x})$ and $\boldsymbol{Q}(\boldsymbol{x})$), and the long term behavior (i.e., $V(\boldsymbol{x})$) is learned by a different procedure.

Acknowledgments

This research was supported by a grant from Boeing Computer Services under Contract W–300445. The authors would like to thank Vangelis Coutsias, Tom Caudell, Don Hush, and Bill Horne for stimulating discussions and insightful suggestions.

References

Cohen, M. (1992). The construction of arbitrary stable dynamics in nonlinear neural networks. *Neural Networks*, *5*(1), 83–103.

Franks, J. (1982). *Homology and dynamical systems*, Vol. 49 of *Regional Conference Series in Mathematics*. American Mathematical Society, Providence, RI.

Howse, J. (1995). *Gradient and Hamiltonian dynamics: Some applications to neural network analysis and system identification*. Ph.D. thesis, University of New Mexico, Department of Electrical Engineering.

LaSalle, J., & Lefschetz, S. (1961). *Stability by Lyapunov's direct method, with applications* (1st edition)., Vol. 4 of *Mathematics in Science and Engineering*. Academic Press, Inc., New York, NY.

Mendes, R., & Duarte, J. (1981). Decomposition of vector fields and mixed dynamics. *Journal of Mathematical Physics*, *22*(7), 1420–1422.

Morgan, A., & Narendra, K. (1977). On the stability of non-autonomous differential equations $\dot{x} = [A + B(t)]x$ with skew-symmetric matrix $B(t)$. *SIAM Journal of Control and Optimization*, *15*(1), 163–176.

Narendra, K., & Annaswamy, A. (1987). Persistent excitation in adaptive systems. *International Journal of Control*, *45*(1), 127–160.

Narendra, K., & Annaswamy, A. (1989). *Stable adaptive systems*. Prentice-Hall, Inc., Englewood Cliffs, NJ.

Varaiya, P., & Liu, R. (1966). Bounded-input bounded-output stability of nonlinear time-varying differential systems. *SIAM Journal on Control*, *4*(4), 699–704.

Willems, J. (1970). *Stability theory of dynamical systems*. John Wiley & Sons, Inc., New York, NY.

Appendix: Proofs

***Proof of Theorem* 3.2**

The following lemma, which is proved in the reference, is used in the proof of this theorem.

Lemma A.1 (LaSalle and Lefschetz (1961)). *Let $V(\boldsymbol{x})$ be a scalar function which for all $\boldsymbol{x}$ has continuous first partial derivatives with the property that $\lim_{\|\boldsymbol{x}\|\to\infty} V(\boldsymbol{x}) \to \infty$. If $\dot{V}(\boldsymbol{x}) \leq -\epsilon < 0$ for all $\boldsymbol{x}$ outside some closed and bounded set $\mathcal{M}$, then the solutions of $\dot{\boldsymbol{x}} = \boldsymbol{f}(\boldsymbol{x}, t)$ are ultimately bounded.*

Proof. Since $\boldsymbol{h}(\cdot)$ is continuous, $\|\boldsymbol{u}(t)\| \leq \mathcal{U} \Rightarrow \|\boldsymbol{h}(\boldsymbol{u}(t))\| \leq \tilde{\mathcal{U}}$. It is given that $\|\nabla_{\boldsymbol{x}} V(\boldsymbol{x})\| \geq \mathcal{K}_u$. Choose $\mathcal{K}_u$ to be

$$\|\nabla V\| \geq \mathcal{K}_u = \frac{\tilde{\mathcal{U}} + \sqrt{\tilde{\mathcal{U}}^2 + 4\,\lambda_{min}\,\epsilon}}{2\,\lambda_{min}},$$

where ϵ is a positive constant and λ_{min} is the smallest eigenvalue of $\boldsymbol{P}(\boldsymbol{x})$ in the region where $\|\boldsymbol{x}\| > \mathcal{F}_u$. Since $\boldsymbol{P}$ is symmetric positive definite, the smallest eigenvalue λ_{min} is real and positive.

$$\therefore \lambda_{min}\,\|\nabla V\|^2 - \|\nabla V\|\,\tilde{\mathcal{U}} - \epsilon \geq 0$$

It is given that $\|\boldsymbol{h}\| \leq \tilde{\mathcal{U}} \Rightarrow -\|\boldsymbol{h}\| \geq -\tilde{\mathcal{U}}$

$$\therefore \lambda_{min}\,\|\nabla V\|^2 - \|\nabla V\|\,\|\boldsymbol{h}\| - \epsilon \geq \lambda_{min}\,\|\nabla V\|^2 - \|\nabla V\|\,\tilde{\mathcal{U}} - \epsilon \geq 0$$

By the Cauchy-Schwarz inequality $\|\nabla V\|\,\|\boldsymbol{h}\| \geq |\nabla V^\dagger\,\boldsymbol{h}|$

$$\therefore \lambda_{min}\,\|\nabla V\|^2 - |\nabla V^\dagger\,\boldsymbol{h}| - \epsilon \geq \lambda_{min}\,\|\nabla V\|^2 - \|\nabla V\|\,\|\boldsymbol{h}\| - \epsilon,$$

where $|\cdot|$ is the absolute value. For the absolute value $|\nabla V^\dagger\,\boldsymbol{h}| \geq \nabla V^\dagger\,\boldsymbol{h}$

$$\therefore \lambda_{min}\,\|\nabla V\|^2 - \nabla V^\dagger\,\boldsymbol{h} - \epsilon \geq \lambda_{min}\,\|\nabla V\|^2 - |\nabla V^\dagger\,\boldsymbol{h}| - \epsilon$$

Since λ_{min} is the smallest eigenvalue of the matrix $\boldsymbol{P}(\boldsymbol{x})$

$$\therefore \nabla V^\dagger\,\boldsymbol{P}\,\nabla V - \nabla V^\dagger\,\boldsymbol{h} - \epsilon \geq \lambda_{min}\,\nabla V^\dagger\,\nabla V - \nabla V^\dagger\,\boldsymbol{h} - \epsilon \geq 0$$
$$\Rightarrow -\nabla V^\dagger\,\boldsymbol{P}\,\nabla V + \nabla V^\dagger\,\boldsymbol{h} \leq -\epsilon$$

The quantity on the left side of the inequality is precisely $\dot{V}(\boldsymbol{x})$ for Equation (9). Therefore $\|\nabla_{\boldsymbol{x}} V(\boldsymbol{x})\| \geq \mathcal{K}_u \Rightarrow \dot{V}(\boldsymbol{x}) \leq -\epsilon$ for all $\boldsymbol{x}$ such that $\|\boldsymbol{x}\| > \mathcal{F}_u$.

It is well known from real analysis that $\int \|\nabla V\|\,d\boldsymbol{x} \geq \|\int \nabla V\,d\boldsymbol{x}\|$.

$$\therefore \int \|\nabla V\|\,d\boldsymbol{x} \geq \left\|\int \nabla V\,d\boldsymbol{x}\right\| > \left\|\int \mathcal{K}_u\,d\boldsymbol{x}\right\|$$
$$\Rightarrow \|V + c\| > \|\mathcal{K}_u\,\boldsymbol{x}\|$$

By Minkowski's inequality $\|V\| + \|c\| \geq \|V + c\|$,

$$\therefore \|V\| + \|c\| \geq \|V + c\| > \mathcal{K}_u \|\boldsymbol{x}\|$$

Since $V \geq 0$ and since V and c are scalars

$$\therefore V > \mathcal{K}_u \|\boldsymbol{x}\| - |c|$$

Hence $\|\nabla_{\boldsymbol{x}} V(\boldsymbol{x})\| \geq \mathcal{K}_u \Rightarrow V(\boldsymbol{x}) > \mathcal{K}_u \|\boldsymbol{x}\| \Rightarrow \lim_{\|\boldsymbol{x}\| \to \infty} V(\boldsymbol{x}) \to \infty$. Note that the converse of this implication is *not* true. Using these two results, it follows immediately from Lemma A.1 that the solutions $\boldsymbol{x}(t)$ of Equation (9) are ultimately bounded. ♦